Exp Brain Res (2010) 202:561–570
DOI 10.1007/s00221-010-2159-9

RESEARCH ARTICLE

Correlation of visual-evoked hemodynamic responses and potentials in human brain

Tiina Näsi · Kalle Kotilahti · Tommi Noponen · Ilkka Nissilä · Lauri Lipiäinen · Pekka Meriläinen

Received: 3 April 2009 / Accepted: 4 January 2010 / Published online: 20 January 2010

Abstract The interaction of brain hemodynamics and neuronal activity has been intensively studied in recent years to yield better understanding of brain function. We investigated the relationship between visual-evoked hemodynamic responses (HDRs), measured with near-infrared spectroscopy (NIRS), and neuronal activity in humans, approximated with the stimulus train duration or with visual-evoked potentials (VEPs). Concentration changes of oxyhemoglobin (HbO_2) and deoxyhemoglobin (HbR) in tissue and VEPs were recorded simultaneously over the occipital lobe of ten healthy subjects to 3, 6, and 12 s pattern-reversing checkerboard stimulus trains having a reversal frequency of 2 Hz. We found that the area-under-the-curves (Σ) of HbO_2 and HbR were linearly correlated with the stimulus train duration and with the ΣVEP summed over the 3, 6, and 12 s stimulus train durations. The correlation was stronger between the ΣHbO_2 or the ΣHbR and the ΣVEP than between the ΣHbO_2 or the ΣHbR and the stimulus train duration. The ΣVEPs explained 55% of the ΣHbO_2 and 74% of the ΣHbR variance, whereas the stimulus train duration explained only 45% of the ΣHbO_2 and 51% of the ΣHbR variance. We used Σ of the NIRS responses and VEPs because we wanted to incorporate all possible processes (e.g., attention, habituation, etc.) affecting the responses. The results indicate that the relationship between brain HDRs and VEPs is approximately linear for 3–12 s long stimulus trains consisting of checkerboard patterns reversing at 2 Hz. To interpret hemodynamic responses, the measurement of evoked potentials is beneficial compared to the use of indirect parameters such as the stimulus duration. In addition, interindividual differences in the HbO_2 and HbR responses may be partly explained with differences in the VEPs.

Keywords Near-infrared spectroscopy · Electroencephalography · Visual-evoked potential · Linear model · Correlation

T. Näsi (✉) · K. Kotilahti · I. Nissilä · L. Lipiäinen · P. Meriläinen
Department of Biomedical Engineering and Computational Science, School of Science and Technology, Aalto University, P.O. Box 12200, 00076 Aalto, Finland
e-mail: tiina.nasi@tkk.fi

T. Näsi · K. Kotilahti
BioMag Laboratory, HUSLAB, Hospital District of Helsinki and Uusimaa, Helsinki University Central Hospital, Helsinki, Finland

T. Noponen
Turku PET Centre, Turku University Hospital, Turku, Finland

Introduction

Electroencephalography (EEG), the measurement of scalp electrical potential differences originating mainly from postsynaptic currents of signaling neurons, is a traditional method for the measurement of brain function. Some modern methods, such as, functional magnetic resonance imaging (fMRI), positron emission tomography (PET), and near-infrared spectroscopy (NIRS), differ from EEG and other electrophysiological methods in that they measure hemodynamic changes related to brain activity. Hemodynamic imaging is possible because the underlying neuronal activity is linked to brain hemodynamics through the so-called neurovascular coupling (NVC) (Fox et al. 1988; Raichle and Mintun 2006). To better understand the results from these techniques, the relationship between neuronal

activity and hemodynamic responses (HDRs) has been studied intensively in recent years. Studies in humans suggest that, under certain circumstances, the HDR is linearly coupled to a stimulus parameter that can be, e.g., the stimulus duration, frequency, or intensity and that roughly approximates the neuronal activity induced by the stimulus (Boynton et al. 1996; Soltysik et al. 2004; Wobst et al. 2001). In this context, linearity means that scaled and summed neuronal activity or stimulus parameter produces scaled and summed HDRs. Mathematically expressed, if $h_1(t)$ and $h_2(t)$ are the HDRs produced by the neuronal activities $n_1(t)$ and $n_2(t)$, respectively, then the HDR to $a\ n_1(t) + b\ n_2(t)$ is $a\ h_1(t) + b\ h_2(t)$, where a and b are scaling factors. In many situations, however, the HDRs do not follow this linear relationship. For instance, HDRs are nonlinearly coupled to visual stimulus contrasts (e.g., Michelson contrast) and concentration changes of oxyhemoglobin (HbO_2) to visual stimulus train durations (Boynton et al. 1996; Rovati et al. 2007; Wobst et al. 2001).

Electrophysiological measurements can predict the neuronal activity more realistically than a simple stimulus parameter, such as the duration, frequency, or intensity, as the stimulus and the evoked neuronal activity may be nonlinearly related. Combined electrophysiological and hemodynamic measurements have mainly been carried out in animals (Devor et al. 2003; Franceschini et al. 2008; Logothetis et al. 2001), but also some human studies have been published (Janz et al. 2001; Obrig et al. 2002; Ou et al. 2008; Rovati et al. 2007). They report both linear and nonlinear relationships between neuronal responses and HDRs, depending on the stimulus type and parameters and the electrophysiological method.

Simultaneous measurement of electrical and vascular brain activity is technically challenging, especially in human subjects. For example, fMRI, using high magnetic fields and changing field gradients, cannot be combined with magnetoencephalography (MEG), which is very sensitive to external magnetic fields. A combined fMRI/EEG measurement is possible but difficult (Bonmassar et al. 1999, 2001; Janz et al. 2001). In contrast to fMRI, NIRS does not affect nor is affected by the electromagnetic fields measured or produced by other techniques and is therefore well-suited for multimodal studies. Compared to fMRI, NIRS has a poorer spatial resolution but a higher temporal resolution and it can measure both HbO_2 and deoxyhemoglobin concentration changes (HbR), whereas the blood-oxygen-level-dependent (BOLD) signal of fMRI is mostly sensitive to HbR. Some simultaneous NIRS and EEG measurements have already been reported in humans (Herrmann et al. 2008; Horovitz and Gore 2004; Kennan et al. 2002; Koch et al. 2006, 2008; Moosmann et al. 2003; Noponen et al. 2005; Obrig et al. 2002; Rovati et al. 2007). However, only Obrig et al. (2002) and Rovati et al. (2007) have attempted to model the relationship between the evoked potentials and the HDRs among these studies.

Currently, there is no clear evidence whether NIRS responses evoked by short (3–12 s) visual stimuli of different durations are linearly correlated with visual-evoked potentials (VEPs) in humans and in animals, or not. Wobst et al. (2001) have shown that HbR responses are linearly coupled to the pattern-reversing (10 Hz) checkerboard stimulus duration (6–24 s) in humans, but HbO_2 responses are not. Furthermore, Obrig et al. (2002) have provided evidence that the relative amplitudes of NIRS responses and VEPs habituate approximately the same amount during a long (1 min) pattern-reversing stimulus, suggesting a linear relationship between them. Our study combines a NIRS measurement of HbO_2 and HbR responses to short (3–12 s) visual stimuli with a simultaneous EEG measurement of VEPs in humans. The area-under-the-curves of VEPs summed over the stimulus train duration (ΣVEP) provide alternative and more direct estimates of neuronal activity in addition to the stimulus train durations. Using area-under-the-curves of NIRS responses and VEPs, we try to incorporate not only habituation but also other processes, such as attention, gaze fixation, and eye movements, affecting the responses. Our hypothesis is that the linear correlation of the HbO_2 and HbR responses is stronger with the ΣVEP as a regressor than with the stimulus train duration as a regressor indicating a more linear relationship between these.

Materials and methods

Instrumentation

We used a 16-channel frequency-domain NIRS instrument which utilized two laser diodes (685 and 830 nm) modulated at 100 MHz as light sources (Nissilä et al. 2005b). Two source fibers transmitted the light with an optical power of 10–15 mW to the subject's head. The light scattered and absorbed in the tissue was guided from the head to detectors (photomultiplier tubes) through 16 fiber bundles.

We recorded VEPs with a 60-channel EEG device (eXimia EEG, Nexstim Ltd.) with a sampling frequency of 1,450 Hz per channel and a passband of 0.1–350 Hz. Eye movements were monitored with an electrooculogram (EOG) for which one electrode was placed laterally and another electrode superiorly to the right eye.

For simultaneous NIRS/EEG measurements, we integrated NIRS fiber holders into the EEG cap (Fig. 1). One NIRS source fiber and eight detector fiber bundles were attached over the occipital lobe on each hemisphere in two semicircles at 2 and 4 cm source-to-detector (SD) distances

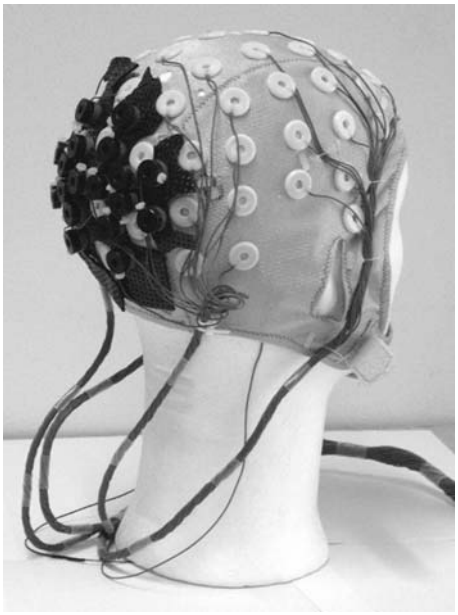

Fig. 1 EEG cap with integrated NIRS fiber holders

(Fig. 2a). A source fiber above each hemisphere was used to avoid disturbances in the optical signals caused by the longitudinal fissure and the superior sagittal sinus. In addition, the two SD distances provided signals that contained differing contributions from superficial and brain tissues (Firbank et al. 1998; Germon et al. 1998).

EEG was recorded mainly above the occipital lobe with 22 Ag/AgCl electrodes (Fig. 2b). The reference electrode was placed on the left cheek, but the data were afterwards rereferenced to Fz (International 10–20 System) to obtain standardized waveforms (American Clinical Neurophysiology Society 2006a; Odom et al. 2004).

An anesthesia monitor (AS/3 Anesthesia Monitor, Datex-Ohmeda, Finland) recorded pulse waveform and arterial oxygen saturation with a pulse oximeter placed on the finger tip and head movements with an inclinometer attached on the forehead.

Subjects

We measured ten healthy male subjects (age 20–36, mean 25.3), who gave their signed informed consent before their enrollment for the study.

Study design

The subjects sat comfortably in a dimmed room during the measurements. They looked at a reversing checkerboard pattern projected on a screen at a 1.5-m distance from their eyes (Fig. 3). The size of the checkerboard pattern was 31.5 × 31.5 cm (12° of the visual field), and each check was 1.3 × 1.3 cm (0.5° of the visual field). A pattern-reversing stimulus was selected, since its VEPs vary less across subjects compared to other typical visual stimuli, and the VEP waveform contains the clearly detectable peaks N75, P100, and N135 (Odom et al. 2004).

Three stimulation runs of about 14 min were presented to each subject with the Presentation® software (version 9.30, http://www.neurobs.com), each followed by rest periods of about 10 min during which the subjects could move (see Fig. 4). Each stimulation run began with a gray screen visible for 30 s, followed by 22 stimulus trains. Each train consisted of 3, 6, or 12 s checkerboard stimulus reversing at 2 Hz and a randomized inter-stimulus-interval (ISI) of 25–35 s (mean 30 s) during which the screen was

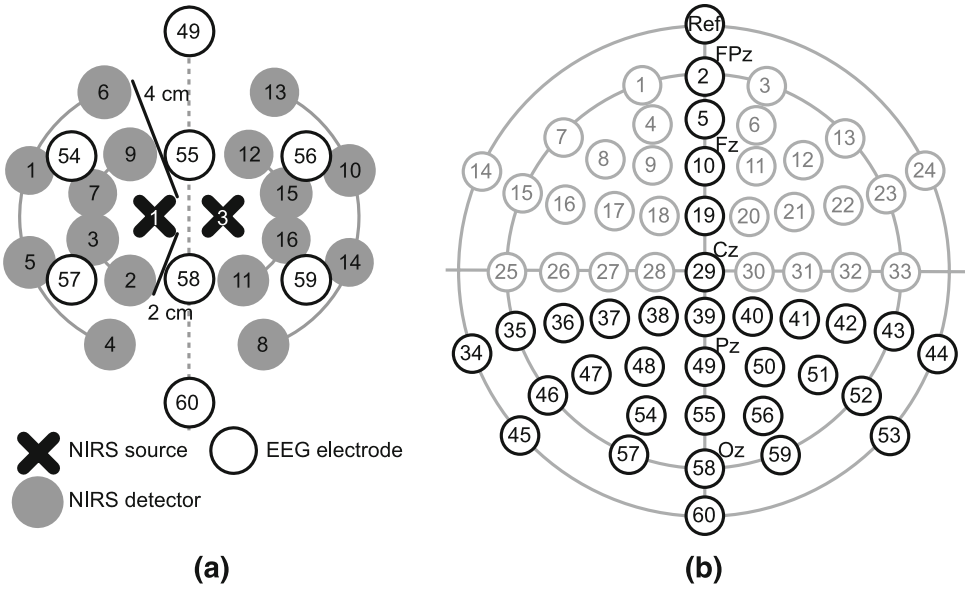

Fig. 2 **a** Layout of NIRS sources and detectors along with some electrodes in the occipital areas. **b** Layout of EEG electrodes. Recorded channels are marked in *black*, other channels in *gray*. Some electrodes are labeled according to the International 10–20 electrode positioning system

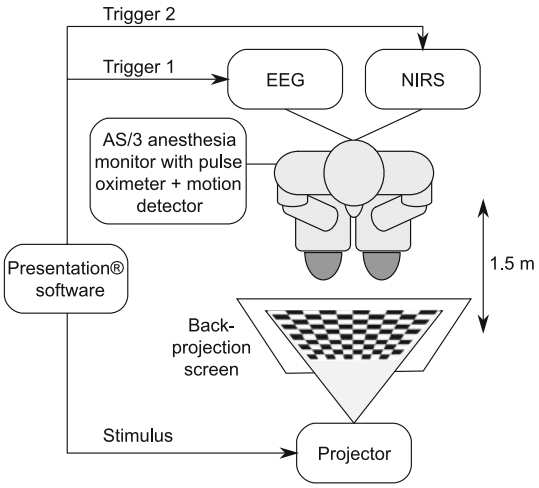

Fig. 3 Measurement set-up

gray. The ISI was randomized to reduce the interference of slow systemic oscillations in the averaged HDRs (Elwell et al. 1999; Obrig et al. 2000), and it was sufficiently long for the HDRs to return back to baseline between the stimulus trains (Dale 1999). Each of the three runs comprised seven 6 and 12 s and eight 3 s stimulus trains in a randomized order. The checkerboard pattern and the gray screen had a small red fixation cross in the center on which the subjects were asked to focus their eyes. Each run contained 278 pattern reversals, resulting in total of 834 pattern reversals for each subject.

The study protocol was approved by the Ethics Committee of the Helsinki University Central Hospital, and it was in compliance with the Declaration of Helsinki.

Data processing (NIRS)

The NIRS amplitude and phase signals were calibrated before further data processing (Nissilä et al. 2005b; Tarvainen et al. 2005). Systemic slow oscillations and fiber contact variations were suppressed by dividing the amplitude signals with low-pass filtered signals (−3 dB cutoff frequency at 0.017 Hz). Higher frequency components, such as the heart beat, were attenuated with low-pass filtering (−3 dB cutoff frequency at 0.33 Hz). Changes in the modulation amplitude of the light were transformed into changes in HbO_2 and HbR with the modified Beer–Lambert law, where the optical path length was determined from the calibrated phase (Elwell 1995). Channels having a standard deviation of the HbO_2 signal higher than 1.7 μM or a standard deviation of the HbR signal higher than 0.7 μM were rejected, since their SNR was not sufficiently high to detect the HDRs. The low SNR of these channels was probably due an excess of hair between the skin and the detector. Epochs containing movements were rejected from the NIRS data using the inclinometer data. Also, epochs containing over 5 μM HbO_2 or 2 μM HbR peak-to-peak changes in the time window from −5 to 25 s with respect to the stimulus onset were rejected because they most likely contained movement or contact artifacts and no reliably detectable HDRs.

The HbO_2 and HbR changes of each subject were averaged for each detector channel and each stimulus train duration in the time window from −5 to 25 s with respect to the stimulus onset. These averaged HDRs of each channel and stimulus train duration were tested with a two-tailed Student's *t* test for statistically significant differences between the mean of the baseline (from −5 to 0 s) and the positive peak value of HbO_2 and negative peak value of HbR in the time window from 4 to 20 s. The significance level was set at 0.05. Channels with statistically significant HbO_2 and HbR responses to a stimulus train duration were accepted for the linearity analysis.

The area-under-the-curves of rectified HbO_2 and HbR responses (ΣHbO_2 and ΣHbR) were calculated for the accepted channels in the time window from the stimulus onset to the return of the HDRs to baseline to quantify the

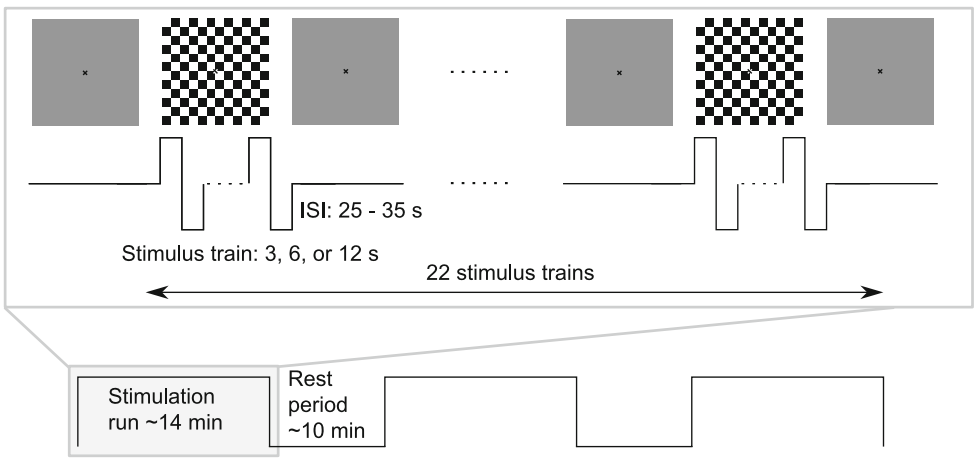

Fig. 4 Stimulation protocol. Three stimulation runs of approximately 14 min were presented to each subject interleaved with approximately 10-min rest periods. The stimulation runs consisted of trains of reversing checkerboard patterns and a gray screen during the ISIs

vascular changes produced by the three different stimuli. Area-under-the-curves were used instead of peak values of the responses, since the response amplitudes saturate when long stimuli are used. The ΣHbO_2 and ΣHbR to different stimuli were not calculated with a fixed time window, since the responses to shorter stimulus trains return faster to baseline than the responses to longer stimulus trains. If the time window was fixed, the ΣHbO_2 and ΣHbR to short stimulus trains would be overestimated because of nonzero noise at the end of the rectified responses. The time point at which the HDR returned to baseline was determined manually for each subject and stimulus separately.

A time-locked average of the heart rate calculated in the time-window from −5 to 25 s from the pulse oximeter data provided an estimate of average systemic changes in the circulation due to stimulation. It was used to ensure that HDRs are evoked by local cerebrovascular changes rather than by global changes in circulation. The data of subjects having greater than 3 bpm changes in their average heart rate were rejected from the data analysis.

Data processing (EEG)

The EEG data were divided into epochs ranging from −100 to 400 ms with respect to each pattern reversal and the initial display of the checkerboard pattern at the start of each stimulus train. Epochs containing eye blinks or clear motion artifacts were rejected, and the mean value of the baseline of the remaining epochs (from −100 to 0 ms) was shifted to zero. The accepted epochs were averaged and band-pass filtered (−3 dB cutoff frequencies at 0.6 and 106.5 Hz).

The VEPs corresponding to the first checkerboard display and to each of the subsequent pattern reversal in the stimulus trains were averaged across the stimulus trains for each channel and subject, resulting in a sequence of averaged VEPs (VEP^i, i = 1, ..., 24, where 24 is the number of consecutive VEPs in the sequence). A higher SNR was obtained for VEPs from VEP^1 to VEP^6, since they were evoked by stimuli present in all of the 3, 6, and 12 s trains. Progressively fewer responses were averaged for the later pattern reversals in the longer trains. Also, a grand average VEP (VEP_{ave}) over all shown pattern reversals (not including the initial display of the pattern, i.e., VEP^1) was calculated for each subject and channel separately.

To minimize noise, the VEP_{ave} was fitted to VEP^i (i = 2, ..., 24) by scaling and latency shifting it. The VEP^1 was left out from the fitting because it is a response to a flash stimulus; the checkerboard showed up from the gray background at the beginning of each stimulus train. This original VEP^1 and a sequence of scaled and latency shifted VEP_{ave} (VEP^i_{ave}, i = 2, ..., 24) were used in subsequent analysis instead of VEP^i (i = 1, ..., 24), since the original VEP^i sequence had a variable and low SNR depending on i. The fitting procedure allowed the VEP^i_{ave} to change in amplitude and latency but not in waveform, which was a reasonable assumption, since the stimulus was unchanged over time.

The fitting procedure of VEP_{ave} to VEP^i was performed so that first a latency shifted $VEP_{ave}(t)$ was calculated for each pattern reversal (i = 2, ..., 24):

$$VEP^i_{ave,\tau}(t) = VEP_{ave}(t - \tau_i), \quad (1)$$

where t is the time index and τ_i the latency shift corresponding to the ith pattern reversal. The parameter τ_i was defined as the time index that maximized the unbiased estimate of the cross-correlation $r(t)$ between $VEP^i(t)$ and $VEP_{ave}(t)$:

$$\tau_i = \underset{t\in[-T+1\ T-1]}{\arg\max}\ r(t), \quad (2)$$

where T is the number of time samples in $VEP^i(t)$.

After latency shifting, the final $VEP^i_{ave}(t)$ was obtained by scaling the $VEP^i_{ave,\tau}(t)$ $VEP^i_{ave,}\tau(t)$ to match its amplitude with the amplitude of the original sequence $VEP^i(t)$:

$$VEP^i_{ave}(t) = a_i VEP^i_{ave,\tau}(t) + b_i, \quad (3)$$

where a_i and b_i are scaling factors obtained by minimizing the sum of squared residuals between $VEP^i(t)$ and $VEP^i_{ave}(t)$ in the time window from 20 to 150 ms. This time window was selected, since it contains all of the three commonly known peaks N75, P100, and N135 of the pattern-reversal VEPs (American Clinical Neurophysiology Society 2006b).

To quantify the magnitude of the VEPs, the area-under-the-curves of rectified VEP^i_{ave} (i = 2, ..., 24) and VEP^1 (ΣVEP^i_{ave} and ΣVEP^1) were calculated separately for each subject and channel in the time window from 0 to 400 ms. Time windows of less than 400 ms were also tested, but the length of the time window had no significant effect on the results. The ΣVEP^i_{ave} and ΣVEP^1 were averaged over electrodes 54–60 (Fig. 2b) and summed over the stimulus train duration to quantify the mean evoked potential activity induced by each of the three stimulus trains. In other words, these sums over the stimulus train durations (ΣVEP) were obtained for the different stimulus train durations as follows:

$$3\,\text{s}: \Sigma VEP = \Sigma VEP^1 + \sum_{i=2}^{6} \Sigma VEP^i_{ave}$$

$$6\,\text{s}: \Sigma VEP = \Sigma VEP^1 + \sum_{i=2}^{12} \Sigma VEP^i_{ave}$$

$$12\,\text{s}: \Sigma VEP = \Sigma VEP^1 + \sum_{i=2}^{24} \Sigma VEP^i_{ave}$$

where ΣVEP^1 and ΣVEP^i_{ave} are the averages over electrodes from 54 to 60.

We also used the difference between amplitudes of P100 and N135 peaks to quantify the evoked potential activity [adopted from Obrig et al. (2002)], but these did not qualitatively change the results.

Linearity

The linearity between the ΣHbO_2 or the ΣHbR and the stimulus train duration or the ΣVEP was measured by fitting a regression line $y = \beta_0 x + \beta_1$ to the data in the least-squares sense, where y is the ΣHbO_2 or the ΣHbR evoked by the stimulus train and x the stimulus train duration or the corresponding ΣVEP. The constants β_0 and β_1 are obtained from the fitting procedure. The regression was performed for each subject separately with y containing all the statistically significant ΣHbO_2s or ΣHbRs of the subject and for all subjects together with y containing the mean over statistically significant ΣHbO_2s or ΣHbRs of each subject. Also, the Pearson's correlation coefficients (r) were calculated and tested with one-sample t test for a null hypothesis that r is zero (data uncorrelated) against an alternative hypothesis that r is not zero (data correlated). The squares of the correlation coefficients—the coefficients of determination (R^2)—were also obtained to quantify the fraction of the variance in y explained by the regression model.

Results

NIRS data

The data of two subjects (subjects 2 and 8) were rejected from further analysis, since in these subjects, the stimulation trains induced over 3 bpm changes in the heart rate. Over all subjects, the stimulation trains induced a change of 2.2 ± 0.3 (mean ± SEM) bpm in the heart rate.

Statistically significant HDRs to at least one of the three stimulus train durations appeared in the NIRS data of the remaining eight subjects (Table 1). Five of these subjects produced statistically significant HbO_2 and HbR responses to all three durations, one to two durations, and two to one duration. The long SD-distance channels had more statistically significant HDRs than the short SD-distance channels during all stimulus train durations. The subjects with responses to only one or two stimulus train durations (subjects 3, 4, and 7) were left out from the further analysis since no regression line could be fitted in their data reliably.

The averages over all statistically significant HDRs of the five accepted subjects (subjects 1, 5, 6, 9, and 10) to each of the three stimulus train durations are shown in Fig. 5. The mean peak amplitudes of statistically significant HbO_2 responses of the accepted subjects were larger than the absolute mean peak amplitudes of the HbR responses, and the shortest stimulus train duration produced lower amplitudes than the two longer ones (Table 2). The ΣHbO_2, ΣHbR and the peak latency of HbO_2 increased with increasing stimulus duration.

Table 1 Numbers of NIRS detector channels having statistically significant HDRs to different stimulus train durations for all accepted subjects

Subject	3 s	6 s	12 s
1	1 (0 + 1)	3 (0 + 3)	2 (0 + 2)
3	2 (1 + 1)	0 (0 + 0)	0 (0 + 0)
4	0 (0 + 0)	0 (0 + 0)	2 (0 + 2)
5	12 (7 + 5)	14 (8 + 6)	13 (7 + 6)
6	2 (0 + 2)	7 (1 + 6)	6 (1 + 5)
7	1 (0 + 1)	1 (0 + 1)	0 (0 + 0)
9	2 (0 + 2)	2 (0 + 2)	2 (0 + 2)
10	1 (0 + 1)	1 (0 + 1)	8 (4 + 4)
All	21 (8 + 13)	28 (9 + 19)	33 (12 + 21)

The values in brackets represent short + long SD-distance channels

VEPs

All subjects showed clear N75, P100, and N135 peaks in their VEPs. The grand average VEPs over all subjects are shown in Fig. 6 for occipital channels. The average of ΣVEP values over accepted subjects were 2.8 ± 0.3, 5.7 ± 0.7, and 11.4 ± 0.8 μVs (mean ± SEM) for the 3, 6, and 12 s stimulus train durations, respectively. The values increased approximately linearly with increasing stimulus train duration. The ΣVEP^i_{ave} values to different stimulus train durations are shown in Fig. 5 along with the average HDRs. The ΣVEP^i_{ave} values did not show clear habituation during the stimulation trains.

Linearity

The results of the linear regression are shown in Table 3 and in Fig. 7. With the ΣVEP as a regressor, the correlation coefficients over all subjects were 0.74 for ΣHbO_2 and 0.86 for ΣHbR, and with stimulus train duration as a regressor 0.67 for ΣHbO_2 and 0.72 for ΣHbR. All of these four correlation coefficients differed statistically significantly from zero ($p < 0.05$) indicating that ΣHbO_2 and ΣHbR are correlated with the ΣVEP and the stimulus train duration. The correlation coefficients of ΣHbR were higher than the ones of ΣHbO_2 with both regressors. Of the regressors, the ΣVEP gave higher correlation coefficients than the stimulus duration, and it explained 55% of the ΣHbO_2 and 74% of the ΣHbR variance, whereas the stimulus duration explained only 45% of the ΣHbO_2 and 51% of the ΣHbR variance.

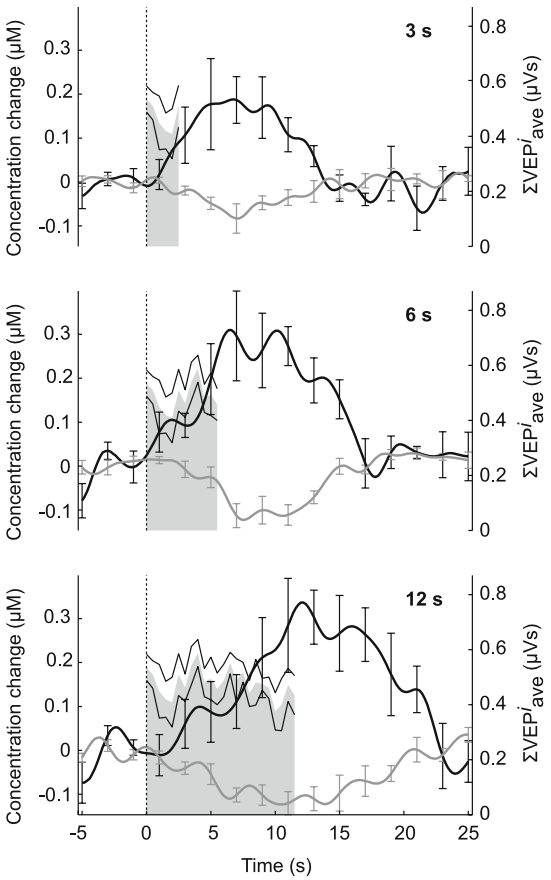

Fig. 5 Mean HbO_2 (*black line*) and HbR (*gray line*) responses over all statistically significant channels of the five subjects accepted into the regression analysis and ΣVEP^i_{ave} (*gray area*) to 3, 6, and 12 s stimulus train durations. *Thin black curves* indicate the SEM of the ΣVEP^i_{ave} and *error bars* the SEM of the HDRs. The *dotted line* indicates stimulus train onset

Table 2 Descriptive statistics of the statistically significant HDRs of accepted subjects (mean ± SEM)

	3 s	6 s	12 s
Mean peak amplitude (μM)			
HbO_2	0.3 ± 0.1	0.4 ± 0.1	0.4 ± 0.1
HbR	−0.11 ± 0.02	−0.13 ± 0.03	−0.14 ± 0.03
Mean peak latency (s)			
HbO_2	8.1 ± 1.5	10.5 ± 1.2	15.3 ± 1.5
HbR	9.8 ± 1.8	9.4 ± 0.8	12.7 ± 2.0
Mean ΣHDR (μMs)			
HbO_2	2.1 ± 0.4	3.6 ± 0.5	4.7 ± 0.7
HbR	0.8 ± 0.1	1.2 ± 0.2	1.9 ± 0.3

The correlation coefficients within subjects (Table 3) showed similar trends as the correlation coefficients over all subjects. The correlation coefficients of ΣHbR were higher than the correlation coefficients of ΣHbO_2 in all cases except subject 6. The improvement in the correlation

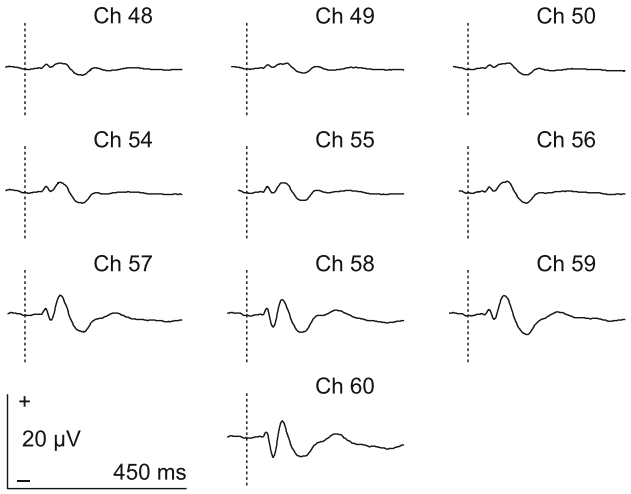

Fig. 6 Grand average VEPs over all subjects over the occipital lobe. The *dotted line* indicates the stimulus onset

coefficients of individual subjects is however small when the regressor is changed from stimulus train duration to ΣVEP. The reason for this is that the correlation coefficients for individual subjects are calculated using all statistically significant channels of the corresponding subject, whereas the correlation coefficients over all subjects are calculated over the ΣHbO2 or ΣHbR values averaged over the statistically significant channels of each subject, resulting in reduced variability in ΣHbO_2 and ΣHbR. Furthermore, there is only one ΣVEP value per stimulus train duration for each subject. When correlation coefficients over all subjects are calculated, the individual ΣVEP values are used, resulting in more than one ΣVEP value per stimulus train duration.

Discussion and conclusions

The main findings of our study are that (1) ΣHbO_2 and ΣHbR correlate linearly with the ΣVEP and the stimulus train duration (3, 6, and 12 s), (2) ΣHbR is more linearly correlated with the stimulus train duration and the ΣVEP than ΣHbO_2 , and (3) the linear correlation of ΣHbO_2 and ΣHbR is stronger with the ΣVEP than with the stimulus train duration.

Our first finding implies that the HDRs are approximately linearly coupled to the stimulus train duration (3–12 s) and the simultaneously measured ΣVEPs. However, according to our second finding, the HbR responses seem to possess a stronger linear relationship with the regressors than the HbO_2 responses. Our third finding implies that there is probably some variability in the neuronal responses caused, e.g., by changes in attention or gaze fixation that is not accounted by the stimulus train

Table 3 Pearson's correlation coefficients (r), their p values [$p(r)$], and coefficients of determination (R^2) separately within all accepted subjects (rows with a subject number) and for all of the accepted subjects together (row 'All')

Subject	ΣVEP						Stimulus duration					
	HbO_2			HbR			HbO_2			HbR		
	r	$p(r)$	R^2	r	$p(r)$	R^2	r	$p(r)$	R^2	r	$p(r)$	R^2
1	0.02	0.967	0.00	0.65	0.165	0.42	−0.04	0.947	0.00	0.69	0.131	0.47
5	0.37	0.022	0.13	0.61	$<10^{-4}$	0.37	0.35	0.030	0.12	0.61	$<10^{-4}$	0.37
6	0.84	$<10^{-3}$	0.70	0.72	0.002	0.52	0.83	$<10^{-3}$	0.70	0.72	0.002	0.52
9	0.61	0.195	0.38	0.95	0.004	0.90	0.61	0.194	0.38	0.95	0.004	0.90
10	0.74	0.015	0.54	0.78	0.008	0.61	0.73	0.016	0.54	0.79	0.006	0.63
All	0.74	0.002	0.55	0.86	$<10^{-4}$	0.74	0.67	0.006	0.45	0.72	0.003	0.51

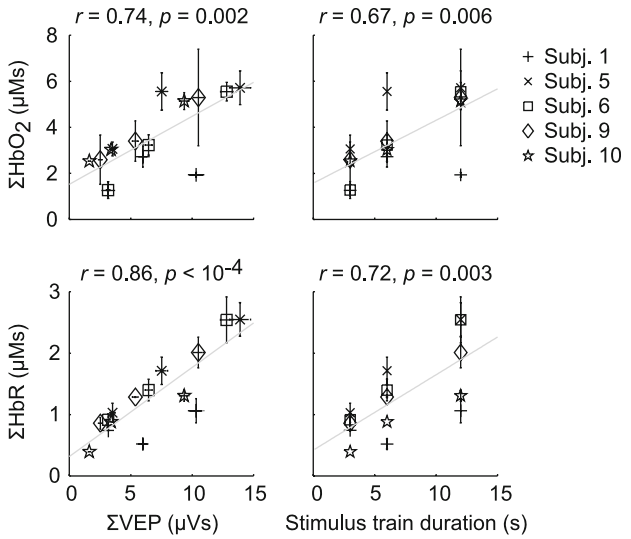

Fig. 7 Average ΣHbO_2 (*upper row*) and ΣHbR (*lower row*) as a function of the ΣVEP (*left*) and a stimulus train duration (*right*) for subjects showing statistically significant HDRs. The *vertical error bars* represent the SEMs of the averaged ΣHbO_2s or ΣHbRs and *horizontal error bars* the SEMs of the ΣVEPs. *Error bars* are not shown for subjects having only one statistically significant HDR for each stimulus train duration. Pearson's correlation coefficient is marked with r and its p value with p. The fitted regression line is shown in *gray*

duration. It also suggests that interindividual differences in HbO_2 and HbR responses may be explained with differences in the evoked potential activity because we calculated the correlation coefficients over the data of all subjects. Thus, a small evoked potential activity of a subject indicates that the ΣHbO_2 and ΣHbR were also probably also small.

The investigation of the NVC with EEG and NIRS includes many challenges. Because these techniques sample partly different volumes, the measured neuronal and hemodynamic signals do not arise from exactly the same area of the brain. The spatial localization of activity sources could be improved by solving the inverse problems from the measurement signals (Arridge 1999; Hämäläinen et al. 1993; Nissilä et al. 2005a).

The visual stimuli used in this study produced relatively weak HDRs, and only five accepted subjects out of eight gave statistically significant positive HbO_2 and negative HbR responses to all three stimulus train durations. Our 2-Hz stimulation frequency was a compromise between a good VEP stimulus and a good NIRS visual stimulus, and in favor of the VEPs. A higher stimulation frequency would have facilitated the detection of HDRs, since their amplitudes increase linearly as a function of the stimulation frequency up to about 8 Hz (Fox and Raichle 1984; Ozus et al. 2001). However, increasing the stimulation frequency would have distorted the VEPs and single VEP waveforms could not have been obtained (American Clinical Neurophysiology Society 2006b). Most of the studies on visual NIRS responses have used a frequency in the range of 6–8 Hz (Plichta et al. 2006, 2007; Rovati et al. 2007; Wobst et al. 2001). To the best of our knowledge, 3 Hz is the lowest frequency of a 1-min pattern-reversing checkerboard stimulus that has previously been reported to evoke HDRs detectable with NIRS (Obrig et al. 2002). Moreover, a moderate reproducibility rate of visual HDRs with an optimal stimulation frequency of 6 Hz has been reported previously (Plichta et al. 2006).

A greater number of presented stimulus trains could have improved the SNR of the HDRs, but increasing the measurement time would have increased the possibility of physiological noise in the signals. Experienced subjects gave more reliable results than first-timers, indicating that breathing, neck tension, attention, etc., may have affected the results of the first-timers through systemic blood flow changes and hemodynamic changes in the superficial layers of the head. Two inexperienced subjects showed increases in their heart rate during the stimulation, which supports this hypothesis. However, activation occurred mostly in long SD-distance channels, suggesting that the measured signals originate mostly from the brain. The channels with a long SD distance should namely sample a greater amount

of brain tissue than the short SD-distance channels (Firbank et al. 1998; Germon et al. 1998).

Despite some challenges in combining NIRS and EEG, we obtained HDRs and VEPs from several subjects. We also confirmed our hypothesis that the linear correlation of ΣHbO_2 and ΣHbR improves when ΣVEPs is used as a regressor instead of the stimulus train duration. In addition, our results are in concordance with previous studies. Wobst et al. (2001) have found that HbR responses are linearly coupled to the stimulus durations of a 10 Hz pattern-reversing checkerboard pattern in the range of 6–24 s. Moreover, BOLD signals, closely related to HbR responses, are linearly coupled to 7.5 and 8 Hz pattern-reversing checkerboard stimulus durations from 3–6 to 24 s (Boynton et al. 1996; Soltysik et al. 2004). Also, the weaker linearity of the HbO_2 response to stimulus duration is in agreement with the results of Wobst et al. (2001).

In conclusion, our study of simultaneous NIRS and EEG measurements in healthy adults suggests that the relationship between brain HDRs and VEPs is approximately linear for 3–12 s long stimulus trains consisting of checkerboard patterns reversing at 2 Hz. However, the results indicate that a linear model is better suited for ΣHbR than ΣHbO_2, and the linear correlations are stronger for the ΣVEP as a regressor than for the stimulus train duration as a regressor. Thus, when interpreting the hemodynamic responses, it is beneficial to relate them to parameters linked to the evoked potentials rather than to indirect parameters (e.g., stimulus duration). In addition, interindividual differences in the HbO_2 or HbR responses to visual stimuli may be explained with interindividual differences in the VEP activity.

Acknowledgments The authors would like to thank Petri Hiltunen for suggestions on regression analysis. We also would like to acknowledge the financial support by the Helsinki University of Technology Training Scholarship, the Finnish Cultural Foundation, the Jenny and Antti Wihuri Foundation, the Instrumentarium Science Foundation, and the Academy of Finland (project 120946).

References

American Clinical Neurophysiology Society (2006a) Guideline 5: Guidelines for standard electrode position nomenclature. J Clin Neurophysiol 23(2):107–110

American Clinical Neurophysiology Society (2006b) Guideline 9b: Guidelines on visual evoked potentials. J Clin Neurophysiol 23(2):138–156

Arridge S (1999) Optical tomography in medical imaging. Inverse Probl 15:R14–R93

Bonmassar G, Anami K, Ives J, Belliveau J (1999) Visual evoked potential (VEP) measured by simultaneous 64-channel EEG and 3T fMRI. NeuroReport 10(9):1893–1897

Bonmassar G, Schwartz D, Liu A, Kwong K, Dale A, Belliveau J (2001) Spatiotemporal brain imaging of visual-evoked activity using interleaved EEG and fMRI recordings. NeuroImage 13(6):1035–1043

Boynton GM, Engel SA, Glover GH, Heeger DJ (1996) Linear systems analysis of functional magnetic resonance imaging in human V1. J Neurosci 16(13):4207–4221

Dale A (1999) Optimal experimental design for event-related fMRI. Hum Brain Mapp 8(2–3):109–114

Devor A, Dunn AK, Andermann ML, Ulbert I, Boas DA, Dale AM (2003) Coupling of total hemoglobin concentration, oxygenation, and neural activity in rat somatosensory cortex. Neuron 39(2):353–359

Elwell CE (1995) A practical users guide to near infrared spectroscopy. UCL, London

Elwell CE, Springett R, Hillman E, Delpy DT (1999) Oscillations in cerebral haemodynamics. Implications for functional activation studies. Adv Exp Med Biol 471:57–65

Firbank M, Okada E, Delpy DT (1998) A theoretical study of the signal contribution of regions of the adult head to near-infrared spectroscopy studies of visual evoked responses. NeuroImage 8(1):69–78

Fox P, Raichle M, Mintun M, Dence C (1988) Nonoxidative glucose consumption during focal physiologic neural activity. Science 241(4864):462–464

Fox PT, Raichle ME (1984) Stimulus rate dependence of regional cerebral blood flow in human striate cortex, demonstrated by positron emission tomography. J Neurophysiol 51(5):1109–1120

Franceschini M, Nissilä I, Wu W, Diamond S, Bonmassar G, Boas D (2008) Coupling between somatosensory evoked potentials and hemodynamic response in the rat. NeuroImage 41(2):189–203

Germon T, Evans P, Manara A, Barnett N, Wall P, Nelson R (1998) Sensitivity of near infrared spectroscopy to cerebral and extracerebral oxygenation changes is determined by emitter–detector separation. J Clin Monit Comput 14:353–360

Hämäläinen M, Hari R, Ilmoniemi RJ, Knuutila J, Lounasmaa OV (1993) Magnetoencephalograpy—theory, instrumentation, and applications to noninvasive studies of the working human brain. Rev Mod Phys 65(2):413–497

Herrmann MJ, Huter T, Plichta M, Ehlis AC, Alpers GW, Muhlberger A, Fallgatter AJ (2008) Enhancement of activity of the primary visual cortex during processing of emotional stimuli as measured with event-related functional near-infrared spectroscopy and event-related potentials. Hum Brain Mapp 29(1):28–35

Horovitz SG, Gore JC (2004) Simultaneous event-related potential and near-infrared spectroscopic studies of semantic processing. Hum Brain Mapp 22(2):110–115

Janz C, Heinrich SP, Kornmayer J, Bach M, Hennig J (2001) Coupling of neural activity and BOLD fMRI response: new insights by combination of fMRI and VEP experiments in transition from single events to continuous stimulation. Magn Reson Med 46(3):482–486

Kennan RP, Horovitz SG, Maki A, Yamashita Y, Koizumi H, Gore JC (2002) Simultaneous recording of event-related auditory oddball response using transcranial near infrared optical topography and surface EEG. NeuroImage 16(3):587–592

Koch SP, Steinbrink J, Villringer A, Obrig H (2006) Synchronization between background activity and visually evoked potential is not mirrored by focal hyperoxygenation: implications for the interpretation of vascular brain imaging. J Neurosci 26(18):4940–4948

Koch SP, Koendgen S, Bourayou R, Steinbrink J, Obrig H (2008) Individual alpha-frequency correlates with amplitude of visual evoked potential and hemodynamic response. NeuroImage 41(2):233–242

Logothetis NK, Pauls J, Augath M, Trinath T, Oeltermann A (2001) Neurophysiological investigation of the basis of the fMRI signal. Nature 412(6843):150–157

Moosmann M, Ritter P, Krastel I, Brink A, Thees S, Blankenburg F, Taskin B, Obrig H, Villringer A (2003) Correlates of alpha rhythm in functional magnetic resonance imaging and near infrared spectroscopy. NeuroImage 20(1):145–158

Nissilä I, Noponen T, Heino J, Kajava T, Katila T (2005a) Diffuse optical imaging. In: Lin J (ed) Advances in electromagnetic fields in living systems, vol 4. Springer, Berlin, pp. 77–130

Nissilä I, Noponen T, Kotilahti K, Katila T, Lipiäinen L, Tarvainen T, Schweiger M, Arridge S (2005b) Instrumentation and calibration methods for the multichannel measurement of phase and amplitude in optical tomography. Rev Sci Instrum 76(4):044302

Noponen T, Kičić D, Kotilahti K, Kajava T, Kähkönen S, Nissilä I, Meriläinen P, Katila T (2005) Simultaneous diffuse near-infrared imaging of hemodynamic and oxygenation changes and electroencephalographic measurements of neuronal activity in the human brain. In: Chance B, Alfano RR, Tromberg B, Tamura M, Sevick-Muraca E (eds) Proceedings of SPIE 5693, pp 179–190

Obrig H, Neufang M, Wenzel R, Kohl M, Steinbrink J, Einhäupl K, Villringer A (2000) Spontaneous low frequency oscillations of cerebral hemodynamics and metabolism in human adults. NeuroImage 12(6):623–639

Obrig H, Israel H, Kohl-Bareis M, Uludag K, Wenzel R, Müller B, Arnold G, Villringer A (2002) Habituation of the visually evoked potential and its vascular response: implications for neurovascular coupling in the healthy adult. NeuroImage 17(1):1–18

Odom JV, Bach M, Barber C, Brigell M, Marmor MF, Tormene AP, Holder GE, Vaegan (2004) Visual evoked potential standard (2004). Doc Opthalmol 108(2):115–123

Ou W, Nissilä I, Radhakrisnan H, Boas DA, Hämäläinen MS, Franceschini MA (2008) Study of neurovascular coupling via simultaneous MEG DOI acquisition. In: Biomedical Optics 2008 Technical Digest, Optical Society of America, Washington DC, p BWC5

Ozus B, Liu HL, Chen L, Iyer MB, Fox PT, Gao JH (2001) Rate dependence of human visual cortical response due to brief stimulation: an event-related fMRI study. Magn Reson Imaging 19(1):21–25

Plichta MM, Herrmann MJ, Baehne CG, Ehlis AC, Richter MM, Pauli P, Fallgatter AJ (2006) Event-related functional near-infrared spectroscopy (fNIRS): are the measurements reliable? NeuroImage 31(1):116–124

Plichta MM, Heinzel S, Ehlis AC, Pauli P, Fallgatter AJ (2007) Model-based analysis of rapid event-related functional near-infrared spectroscopy (NIRS) data: a parametric validation study. NeuroImage 35(2):625–634

Raichle M, Mintun M (2006) Brain work and brain imaging. Annu Rev Neurosci 29:449–476

Rovati L, Salvatori G, Bulf L, Fonda S (2007) Optical and electrical recording of neural activity evoked by graded contrast visual stimulus. BioMed Eng Online 6:28

Soltysik DA, Peck KK, White KD, Crosson B, Briggs RW (2004) Comparison of hemodynamic response nonlinearity across primary cortical areas. NeuroImage 22(3):1117–1127

Tarvainen T, Kolehmainen V, Vauhkonen M, Vanne A, Gibson AP, Schweiger M, Arridge SR, Kaipio JP (2005) Computational calibration method for optical tomography. Appl Opt 44(10):1879–1888

Wobst P, Wenzel R, Kohl M, Obrig H, Villringer A (2001) Linear aspects of changes in deoxygenated hemoglobin concentration and cytochrome oxidase oxidation during brain activation. NeuroImage 13(3):520–530